2miy

NASA TECHNICAL
MEMORANDUM

NASA TM X-64851

DESIGN OF A DIGITAL CONTROLLER FOR
SPINNING FLEXIBLE SPACECRAFT

By B. C. Kuo, S. M. Seltzer, G. Singh, and
    R. A. Yackel
Astrionics Laboratory

April 1974

NASA

George C. Marshall Space Flight Center
Marshall Space Flight Center, Alabama

1. REPORT NO. NASA TM X-64851	2. GOVERNMENT ACCESSION NO.	3. RECIPIENT'S CATALOG NO.
4. TITLE AND SUBTITLE DESIGN OF A DIGITAL CONTROLLER FOR SPINNING FLEXIBLE SPACECRAFT		5. REPORT DATE April 1974
		6. PERFORMING ORGANIZATION CODE
7. AUTHOR(S) B. C. Kuo* S. M. Seltzer,** G. Singh,* and R. A. Yackel *		8. PERFORMING ORGANIZATION REPORT #
9. PERFORMING ORGANIZATION NAME AND ADDRESS George C. Marshall Space Flight Center Marshall Space Flight Center, Alabama 35812		10. WORK UNIT NO.
		11. CONTRACT OR GRANT NO.
		13. TYPE OF REPORT & PERIOD COVERED
12. SPONSORING AGENCY NAME AND ADDRESS National Aeronautics and Space Administration Washington, D. C. 20546		Technical Memorandum
		14. SPONSORING AGENCY CODE

15. SUPPLEMENTARY NOTES
* University of Illinois, Urbana, Ill.
* * George C. Marshall Space Flight Center, Marshall Space Flight Center, Alabama

16. ABSTRACT

A new approach to digital control system design is applied to the analysis and design of a practical onboard digital attitude control system for a class of spinning vehicles characterized by a rigid body and two connected flexible appendages. The approach used is to design a continuous-data control system that will provide a satisfactory system response. Then, using the digital redesign method, a digital controller with onboard digital computer is designed to provide a digital control system whose states are similar to those of the continuous system at sampling instants. The simplicity of application of this approach is indicated by example. The example, using spinning Skylab parameters, is used to substantiate the conclusions.

17. KEY WORDS	18. DISTRIBUTION STATEMENT Unclassified-unlimited

19. SECURITY CLASSIF. (of this report) Unclassified	20. SECURITY CLASSIF. (of this page) Unclassified	21. NO. OF PAGES 33	22. PRICE NTIS

MSFC - Form 3292 (Rev December 1972)   For sale by National Technical Information Service, Springfield, Virginia 22151

TABLE OF CONTENTS

LIST OF ILLUSTRATIONS

A   Matrix associated with $\underline{z}$ in $\underline{z}$ - state eq. and with $\underline{x}$ in $\underline{x}$ - state eq.

B   Matrix associated with $\underline{v}$ in $\underline{z}$ - state eq. and with $\underline{u}$ in $\underline{x}$ - state eq.

CM   Vehicle center of mass

CM_s Nominal spinning steady state location of CM

$\underline{c}$ Vector form CM to CM_s

c $= (1 - K_2)/(1 + K_1)$

D   Damping matrix in second order $\underline{y}$ - state eq.

D^B Structural damping matrix

D(T)   Sampled-data matrix, eq. (3-17)

d_i Structural damping of non-rotating boom in direction of ith axis

dm   Differential mass element of flexible appendages

E   3x3 identity matrix

E_6 6x6 identity matrix

E(0)   mxm forward gain matrix in continuous-data system

E(T)   mxm forward gain matrix in sampled-data system

$E_W(T)$ Weighted E(T)

F   Matrix associated with $\underline{v}$ in second order $\underline{y}$ - state eq.

$\underline{F}^S$ Applied and structural connection force vector acting on m^S

f_1 $= 1/[1 - \gamma_1(1 + \xi^2)]$

f_2 $= 1/(1 - \gamma_3 - \xi^2 \gamma_1 c)$

G(0)   mxn feedback matrix

G(T)   mxn feedback gain matrix in sampled-data system

$G_w(T)$ Weighted G(T)

$\underline{H}$ Angular momentum vector

H   Weighting matrix in sampled-data system

II   Inertia diadic of entire vehicle

I   Moment of inertia matrix of entire vehicle

I_i Principal moment of inertia of entire vehicle about ith vehicle axis

K   Stiffness matrix in second order $\underline{y}$ - state eq.

K_1 $= (I_2 - I_3)/I_1$

K_2 $= (I_3 - I_1)/I_2$

K_e^B Elastic stiffness matrix of attached flexible booms

K_g^B Geometric stiffness matrix of attached flexible booms

k   An integer

k_i Stiffness of non-rotating boom in direction of ith axis

M   Mass matrix in second order $\underline{y}$ - state eq.

m   Mass of each flexible boom's tip mass

m^s sth mass element of flexible appendage

0_{36} 3x6 null matrix

r   Distance of tip mass' center of mass from CM

$\underline{r}^s$ Vector from CM_s to spinning steady state location of m^s

r(t)   mx1 input vector

$\underline{T}$ Applied torque vector

T   Sample period

T_i Applied (control) torque about ith vehicle axis

t_o $= kT$

$\underline{u}$ Forcing function (normalized torque) in $\underline{x}$ - state eq.

u^1, u^2 Displacement of tip masses (of two flexible booms) from their spinning steady locations to their instantaneous locations

$\underline{u}^B$ $= u^1 - u^2$

$\underline{u}^S$ Vector from spinning steady state location of m^S to its instantaneous location

$\underline{u}_c$ Control vector for continuous system

$\underline{u}_c(t)$ mx1 control vector

$\underline{v}$ Forcing function vector

v_i $= T_i / I_i \Omega^2$

w Variation in angular speed

w_i Variation in angular speed about ith vehicle axis

$\underline{X}$ Inertial position vector from an inertially fixed reference point to the instantaneous location of CM

$\underline{x}$ $= [\phi_1, \phi_2, \mu_3, \phi_1', \phi_2', \mu_3']^T$, state vector

$\underline{x}_c(t)$ nx1 state vector

$\underline{y}$ $= [\phi_1, \phi_2, \phi_3, \mu_1, \mu_2, \mu_3]^T$, state vector

$\underline{z}$ $= [\underline{y} \mid \underline{y}']^T$

α_{ij} Control gain associated with T_i, ϕ_j

β_{ij} Control gain associated with T_i, w_j

Γ_i Distance from CM to tip mass along ith vehicle axis

γ_i $= 2m \, \Gamma_2^2 / I_i$

Δ_i $= d_i / m\Omega$

$\theta(T)$ Sampled-data matrix, eq. (3-18)

$\theta_c(T)$ Sampled-data matrix, eq. (3-19)

λ $= (k+1)T - \tau$

μ_i $= (u_i^1 - u_i^2)/2\Gamma_2$

ξ $= \Gamma_3/\Gamma_2$

$\underline{\rho}$ Vector joining spinning steady state location of CM to each m^s

σ_i^2 $= k_i/m\Omega^2$

τ $= \Omega t$

ϕ_j Angular displacement about ith vehicle axis

Ω Nominal spin rate

$\underline{\omega}$ Rotation vector of entire vehicle

T Transpose

$\cdot$ Time derivation in inertial frame

$\circ$ Time derivative in frame fixed to core rigid body

$\prime$ Differentiation with respect to τ

$\sim$ Operator forming skew-symmetric matrix from column matrix

TECHNICAL MEMORANDUM X-64851

DESIGN OF A DIGITAL CONTROLLER FOR SPINNING FLEXIBLE SPACECRAFT

Summary

A new approach to digital control system design is applied to the analysis and de-
sign of a practical onboard digital attitude control system for a class of spinning vehicles
characterized by a rigid body and two connected flexible appendages. The approach used
is to design a continuous-data control system that will provide a satisfactory system re-
sponse. Then, using the digital redesign method, a digital controller with onboard digital
computer is designed to provide a digital control system whose states are similar to those
of the continuous system at sampling instants. The simplicity of application of this ap-
proach is indicated by example. The example, using spinning Skylab parameters, is
used to substantiate the conclusions.

I. Introduction

In 1970, NASA initiated a set of studies of several Skylab configurations, includ-
ing a spinning vehicle configuration. (The spin would provide an artificial-gravity
environment to assess and compare the physiological benefits and problems of prolonged
zero-gravity and artificial-gravity environments.) The study proceeded generally along two
mutually reinforcing directions. In one case, a large-scale digital simulation of the

1

spinning system of connected flexible and rigid structures was developed, first devising a program for obtaining the eigenvalues and eigenvectors and then simulating the truncated equations for motion. (1), (2), (3) In order to develop faith in the response of the large scale simulation and to obtain characteristic numerical values for the control system parameters, a simplified analytically-tractable model was developed and analyzed in detail. (4),(5) While the model was developed to meet Skylab demands, it is applicable to other spinning bodies with flexible attached members. It consists of a single rigid-core body with two attached flexible massless booms having tip masses (Fig. 1-1). Active closed loop attitude control is implemented by applying control torques to the vehicle to compensate for the effect of disturbance torques. (In the Skylab example, existing Skylab onboard sensors and momentum exchange systems are used for generating control error signals and torques.)(6)

The approach used is to design a continuous-data control system that will provide a satisfactory system response. Then using several recently developed techniques, the continuous control system model is redesigned to provide a digital control system. The objective of the digital redesign is to provide a system whose states are identical to those of the continuous system at sampling instants.

II. Equations of Motion

The spinning flexible vehicle is assumed to be modeled as shown in Fig. 1-1. For the entire vehicle, equations of displacement and rotation are written using Newton-Euler relations. The equations are based on the assumption that the axis of maximum moment of inertia of the overall vehicle does not coincide with the desired spin axis -- usually an axis normal to the solar panels and pointed toward the sun. In that case, the overall mass distribution of the system must be altered to align the two axes-hence, the

inclusion of booms (assumed to be massless and flexible) with tip masses. It is assumed that the booms are attached to the core rigid body at the axis of rotation of the overall system. The basic coordinate system's origin is at the steady-state mass center of the overall vehicle, and the axes coincide with the principal axes of inertia of the steady-state configuration of the vehicle. (In steady-state, the vehicle rotates about the major principal axis.)

The nonlinear equation defining the rotational motion of the overall vehicle (Fig. 1-1) is obtained from the Euler relation and becomes

$$\underline{T} = \dot{\underline{H}} = \mathbb{I} \cdot \dot{\underline{\omega}} + \overset{o}{\mathbb{I}} \cdot \underline{\omega} + \underline{\omega} \times \mathbb{I} \cdot \underline{\omega} + \frac{d}{dt} \int \underline{\rho} \times \dot{\underline{\rho}} \ dm \tag{2-1}$$

where $\underline{T}$ is the applied torque vector, $\underline{H}$ is the angular momentum vector, $\mathbb{I}$ is the inertia diadic of the entire vehicle, $\underline{\omega}$ is the rotation vector of the entire vehicle, $\underline{\rho}$ is a generic vector joining the spinning steady-state location of the vehicle center of mass (CM) to each of the mass elements dm of the flexible appendages, the closed overdot ($\cdot$) represents the time derivative in the inertial frame, and the open overdot ($\circ$) represents the time derivative in a frame that is fixed with respect to the core rigid body. The nonlinear equation representing translational motion of each sth mass element (m^S) of the flexible appendages is obtained from the Newton relation and becomes

$$\underline{F}^S = m^S (\ddot{\underline{X}} + \ddot{\underline{c}} + \ddot{\underline{r}}^S + \ddot{\underline{u}}^S)$$

$$= m^S \{\ddot{\underline{X}} + \overset{oo}{\underline{c}} + 2 \underline{\omega} \times \overset{o}{\underline{c}} + \overset{o}{\underline{\omega}} \times \underline{c} + \underline{\omega} \times (\underline{\omega} \times \underline{c}) + \overset{oo}{\underline{r}}^S + \overset{oo}{\underline{u}}^S$$

$$+ 2 \underline{\omega} \times (\overset{o}{\underline{r}}^S + \overset{o}{\underline{u}}^S) + \overset{o}{\underline{\omega}} \times (\underline{r}^S + \underline{u}^S) + \underline{\omega} \times [\underline{\omega} \times (\underline{r}^S + \underline{u}^S)]\} \tag{2-2}$$

where $\underline{F}$ is the applied and structural connection force vector, $\underline{X}$ is the inertial position vector from an inertially fixed reference point to the instantaneous location of the CM, $\underline{c}$ is the vector from the CM to the nominal spinning steady state location of the CM_S, $\underline{r}^S$ is a vector from CM_S to the spinning steady state location of m^S, and $\underline{u}^S$

3

is a vector from the spinning steady state location of m^s to its actual instantaneous location.

If now these equations are linearized as perturbations about the spinning steady state, perturbation equations (2-3) and (2-4) result. Only the rotational relations have been retained, and the effect of the center of mass motion with respect to the body is neglected. The contribution of mass center motion due to flexible appendage motion and orbital dynamics is ignored. The resulting three linearized equations of motion are written explicitly in matrix notation:

$$T = I\dot{w} + \widetilde{\Omega}Iw + \widetilde{w}I\,\Omega + \widetilde{\Omega}I\Omega + m\widetilde{\Omega}\,(2r^{T}u^{B}E - ru^{B^{T}} - u^{B}r^{T})\Omega +$$

$$m(2r^{T}\dot{u}^{B}E - \dot{u}^{B}r^{T} - r\dot{u}^{B^{T}})\Omega + m\widetilde{r}\ddot{u}^{B} + m\widetilde{\Omega}\,\widetilde{r}\dot{u}^{B} \qquad (2\text{-}3)$$

where I is the moment of inertia matrix of the entire vehicle, $\Omega = [\Omega_1, \Omega_2, \Omega_3]^T$ is the nominal spin rate, $w = [w_1, w_2, w_3]^T$ is the variation of spin speed, E is an identity matrix, m is the mass of each flexible boom's tip mass, $u^B = u^1 - u^2$, where u^1 and u^2 represent the displacement of the tip masses of each of the two flexible booms from their spinning steady state location to their instantaneous location, and $r = [0, r_2, r_3]^T$ represents the distance of the tip mass center of mass from the vehicle center of mass. A set of three equations describes the skew symmetric mode of the attached booms and tip masses:

$$m\ddot{u}^{B} + (D^{B} + 2m\widetilde{\Omega})\dot{u}^{B} + (K_e^{B} + m\widetilde{\Omega}\widetilde{\Omega} + K_g^{B})u^{B} - m\widetilde{r}\,\dot{w} + m(\widetilde{\Omega}\,\widetilde{w} + \widetilde{w}\,\widetilde{\Omega})r = 0 \qquad (2\text{-}4)$$

where $K_e^B = \text{diag}\,[k_1, k_2, k_3]$ and K_g^B represent the elastic and geometric stiffness, respectively, of the attached flexible booms (represented as massless cantilever beams with attached discrete tip masses), and $D^B = \text{diag}\,[d_1, d_2, d_3]$ is the structural damping. Stretching of the booms due to centrifugal force is represented by K_g^B.

Active closed loop control is implemented by applying control torques to the vehicle. It is assumed that the 3-axis of the body-fixed coordinate frame must be held fixed in inertial space. This is achieved by applying control torques to the vehicle to

4

compensate for the effect of disturbance torques. These control torques must in some manner depend on error signals that are proportional both to the angle between the 3-axis and the inertial reference vector and to its time derivative. This information can be generated if the spacecraft hardware includes, for example, sun sensors and rate gyros and the sun is used in place of an inertial reference. The sun sensor measure the angular rotations ϕ_1, ϕ_2 (as also indicated for the simplified model of Fig. 1-1), and rate gyros measure the angular velocities w_1, w_2. The control torques T_1, T_2 may be provided by momentum exchange devices such as control moment gyroscopes and augmented if necessary by a mass expulsion system; for simplicity it generally is assumed that $T_3 = 0$. (It is observed that the existing Skylab, which is used as a model to obtain numerical results herein, has onboard sun sensors, rate gyros, CMG's, and a mass expulsion system.)(6) A more complete derivation of the equations of motion is included in Ref. 7.

A linear control postulate (termed Control Law 1) can be formulated as

$$
\begin{bmatrix} T_1 \\ T_2 \end{bmatrix} = \begin{bmatrix} \alpha_{11} & \alpha_{12} \\ \alpha_{21} & \alpha_{22} \end{bmatrix} \begin{bmatrix} \phi_1 \\ \phi_2 \end{bmatrix} + \begin{bmatrix} \beta_{11} & \beta_{12} \\ \beta_{21} & \beta_{22} \end{bmatrix} \begin{bmatrix} w_1 \\ w_2 \end{bmatrix}
\tag{2-5}
$$

where, from kinematic relations,

$$
\begin{bmatrix} w_1 \\ w_2 \\ w_3 \end{bmatrix} = \begin{bmatrix} -1 & 0 & 0 \\ 0 & -1 & 0 \\ 0 & 0 & -1 \end{bmatrix} \begin{bmatrix} \dot{\phi}_1 \\ \dot{\phi}_2 \\ \dot{\phi}_3 \end{bmatrix} + \begin{bmatrix} 0 & \Omega & 0 \\ -\Omega & 0 & 0 \\ 0 & 0 & 0 \end{bmatrix} \begin{bmatrix} \phi_1 \\ \phi_2 \\ \phi_3 \end{bmatrix}
\tag{2-6}
$$

An estimate of numerical values for the control gains may be obtained by an analysis of a simplified model of the vehicle. In that case – as shown subsequently – continuous-data control system gains for the output feedback of Eq. (2-5) may be determined by application of D-decomposition and parameter mapping techniques.(8) Alternately, optimal gains (Control Law 2) may be determined for complete state feedback by a

linear quadratic loss program to minimize a performance index. (9) Then the continuous control system model gains are altered to provide the desired system dynamic response when it is modeled as a digital system.

When Eqs. (2-3), (2-4), and (2-6) are grouped in the conventional manner, the following set of equations results, assuming the steady state spin Ω is about the 3-axis. In this case $K_g^B = \text{diag} [m\Omega^2, 0, m\Omega^2]$.

$$M\underline{y}'' + D\underline{y}' + K\underline{y} = - F\underline{v} \tag{2-7}$$

where ' refers to differentiation with respect to $\tau = \Omega t$,

$$\underline{y} = [\phi_1, \phi_2, \phi_3, \mu_1, \mu_2, \mu_3]^T, \tag{2-8}$$

$$\underline{v} = [v_1, v_2, v_3]^T = [T_1/I_1\Omega^2, T_2/I_1\Omega^2, T_3/I_3\Omega^2]^T \tag{2-9}$$

and matrices M, D, K, and F are given by Eq. (2-10) through (2-13). The symbols used are defined as

$$K_1 = (I_2 - I_3)/I_1, \quad K_2 = (I_3 - I_1)/I_2, \quad \gamma_i = 2\Omega\Gamma_2^2/I_i, \quad \mu_i = (u_i^1 - u_i^2)/2\Gamma_2$$

$$\Delta_i = d_i/m\Omega, \quad \sigma_i^2 = k_i/m\Omega^2, \quad (i = 1, 2, 3), \quad \xi = \Gamma_3/\Gamma_2.$$

In the steady state, the principal axes of inertia of the total vehicle coincide with the 1, 2, 3 axes and the principal moments of inertia are I_1, I_2, I_3, respectively, with $I_1 < I_2 < I_3$. The stiffness of the nonrotating booms in the directions of the 1, 2, 3 axes is represented by k_i and the structural damping by d_i.

$$M = \begin{bmatrix} 1 & 0 & 0 & 0 & \xi\gamma_1 & -\gamma_1 \\ 0 & \dfrac{1+K_1}{1-K_2} & 0 & -\xi\gamma_1 & 0 & 0 \\ -\gamma_1 & 0 & 0 & 0 & 0 & \gamma_1 \\ 0 & 0 & 1 & \gamma_3 & 0 & 0 \\ 0 & -\xi & 1 & 1 & 0 & 0 \\ \xi & 0 & 0 & 0 & 1 & 0 \end{bmatrix} \tag{2-10}$$

$$D = \begin{bmatrix} 0 & -(1+K_1) & 0 & 2\xi\gamma_1 & 0 & 0 \\ 1+K_1 & 0 & 0 & 0 & 2\xi\gamma_1 & 0 \\ 0 & 0 & 0 & 0 & 0 & \gamma_1\Delta_3 \\ 0 & 0 & 0 & 0 & -2\gamma_3 & 0 \\ -2\xi & 0 & 0 & \Delta_1 & -2 & 0 \\ 0 & -2\xi & 2 & 2 & \Delta_2 & 0 \end{bmatrix} \tag{2-11}$$

$$K = \begin{bmatrix} -K_1 & 0 & 0 & 0 & -\xi\gamma_1 & -\gamma_1 \\ 0 & K_2(\frac{1+K_1}{1-K_2}) & 0 & \xi\gamma_1 & 0 & 0 \\ -\gamma_1 & \ell & 0 & 0 & 0 & \gamma_1(\sigma_3^2+1) \\ 0 & 0 & 0 & 0 & 0 & 0 \\ 0 & \xi & 0 & \sigma_1^2 & 0 & 0 \\ -\xi & 0 & 0 & 0 & \sigma_2^2-1 & 0 \end{bmatrix} \tag{2-12}$$

$$F = \begin{bmatrix} 1 & 0 & 0 & 0 & 0 & 0 \\ 0 & 1 & 0 & 0 & 0 & 0 \\ 0 & 0 & 0 & 1 & 0 & 0 \end{bmatrix}^T \tag{2-13}$$

If control is exerted only about the 1- and 3- axes, then

$$F = \begin{bmatrix} 1 & 0 & 0 & 0 & 0 & 0 \\ 0 & 0 & 0 & 0 & 0 & 0 \\ 0 & 0 & 0 & 1 & 0 & 0 \end{bmatrix}^T \tag{2-14}$$

and

$$-M^{-1}F = \begin{bmatrix} -f_1 & 0 & 0 & 0 & \xi f_1 & -f_1 \\ 0 & 0 & 0 & 0 & 0 & 0 \\ 0 & \xi\gamma_1 c f_2 & -(1-\xi^2\gamma_1 c)f_2 & f_2 & 0 & 0 \end{bmatrix}^T \tag{2-15}$$

where

$$f_1 = 1/[1 - \gamma_1(1 + \xi^2)], \tag{2-16}$$

$$f_2 = 1/(1 - \gamma_3 - \xi^2 \gamma_1 c), \tag{2-17}$$

$$c = (1 - K_2)/(1 + K_1) \tag{2-18}$$

Eq. (2-7) may be cast in state equation form:

$$\underline{z}' = A\underline{z} + B\underline{v} \tag{2-19}$$

where

$$\underline{z} = [\underline{y} \mid \underline{\dot{y}}]^T, \tag{2-20}$$

$$A = \left[\begin{array}{c|c} 0 & E_6 \\ \hline -M^{-1}K & -M^{-1}D \end{array}\right] \tag{2-21}$$

$$B = [0_{36} \mid -M^{-1}F] \tag{2-22}$$

and E_6 is the 6 x 6 identity matrix and 0_{36} is the 3 x 6 null matrix.

It has been shown that when Γ_3 is sufficiently small that it may be ignored, the equations of motion (2-7) uncouple into two sets of equations: one describing the wobble motion (described by μ_3 amd w_1, w_2 or φ_1, φ_2) and one describing the in-plane motion (described by μ_1, μ_2, and w_3 or φ_3). (3) The resulting equation for wobble dynamics can be written as

$$\underline{x}' = A\underline{x} + B\underline{u} \tag{2-23}$$

where

$$\underline{x} = [\phi_1, \phi_2, \mu_3, \phi_1', \phi_2', \mu_3']^T \tag{2-24}$$

8

$$A = \begin{bmatrix} 0 & 0 & 0 & 1 & 0 & 0 \\[4pt] 0 & 0 & 0 & 0 & 1 & 0 \\[4pt] 0 & 0 & 0 & 0 & 0 & 1 \\[4pt] \dfrac{K_1+\gamma_1}{1-\gamma_1} & 0 & \dfrac{-\gamma_1\sigma_3^2}{1-\gamma_1} & 0 & \dfrac{1+K_1}{1-\gamma_1} & \dfrac{-\gamma_1\Delta_3}{1-\gamma_1} \\[10pt] 0 & -K_2 & 0 & -(1-K_2) & 0 & 0 \\[10pt] \dfrac{K_1+1}{1-\gamma_1} & 0 & \dfrac{\gamma_1-(\sigma_3^2+1)}{1-\gamma_1} & 0 & \dfrac{1+K_1}{1-\gamma_1} & \dfrac{-\Delta_3}{1-\gamma_1} \end{bmatrix} \qquad (2\text{-}25)$$

For control torque exerted only about the 1-axis,

$$\underline{u} = v_1 = T_1/I_1\Omega^2 \qquad (2\text{-}26)$$

and

$$B = [0, 0, 0, -1/(1-\gamma_1), 0, -1/(1-\gamma_1)]^T \qquad (2\text{-}27)$$

In the design examples that follow, numerical values typical of the spinning Skylab configuration are used and repeated in the table. (3)

Table 2-1

$I_1 = 1.25 \times 10^6 \text{kgm}^2$	$\Gamma_1 = 0$	$m = 227\text{kg}$
$I_2 = 6.90 \times 10^6 \text{kgm}^2$	$\Gamma_2 = 23.3\,\text{m}$	$k_1 = k_3 = 146\text{N/m}$
$I_3 = 7.10 \times 10^6 \text{kgm}^2$	$\Gamma_3 = -1.53\text{m}$	$k_2 = 7.4 \times 10^4 \text{N/m}$
$d_1 = d_3 = 0.04(k_3 m)^{\frac{1}{2}}$	$d_2 = 0.04(k_2 m)^{\frac{1}{2}}$	$\Omega = 0.6\text{s}^{-1}$

III. Digital Approximation by Point-by-Point State Comparison

The problem considered in this paper is that of approximating a continuous-data feedback system by inserting sample-and-hold devices, and then modifying the input and the feedback gains of the system so that the response of the sampled-data model is as close to that of the original system as possible.

Consider that the continuous-data system as shown in Fig. 3-1 is described by the following time-invariant dynamic equations:

$$\dot{\underline{x}}_c(t) = A\underline{x}_c(t) + B\underline{u}_c(t) \tag{3-1}$$

$$\underline{u}_c(t) = E(0)\underline{r}(t) - G(0)\underline{x}_c(t) \tag{3-2}$$

where

$$\underline{x}_c(t) = n \times 1 \text{ state vector}$$

$$\underline{u}_c(t) = m \times 1 \text{ control vector}$$

$$r(t) = m \times 1 \text{ input vector}$$

$$A = n \times n \text{ coefficient matrix}$$

$$B = n \times m \text{ coefficient matrix}$$

$$E(0) = m \times m \text{ forward gain matrix}$$

$$G(0) = m \times n \text{ feedback matrix}$$

The initial state is given by $\underline{x}_c(t_o)$. Substituting Eq. (3-2) into Eq. (3-1) yields

$$\dot{\underline{x}}_c(t) = [A - BG(0)]\,\underline{x}_c(t) + BE(0)\underline{r}(t) \tag{3-3}$$

The solution of Eq. (3-3) for $t \geq t_o$ is

$$\underline{x}_c(t) = e^{[A-BG(0)](t-t_o)}\underline{x}_c(t_o) + \int_{t_o}^{t} e^{[A-BG(0)](t-\tau)}BE(0)r(\tau)d\tau \tag{3-4}$$

where

$$e^{[A-BG(0)](t-t_o)} = \sum_{j=o}^{\infty} \frac{1}{j!}[A - BG(0)]^j (t-t_o)^j \tag{3-5}$$

The block diagram of the sampled-data system which is to approximate the system of Fig. 3-1 is shown in Fig. 3-2. The outputs of the sample-and hold-devices are a series of step functions with amplitudes denoted by $\underline{u}_s(kT)$ for $kT \leq t < (k+1)T$. The notations, G(T) and E(T), denote the feedback gain and the forward gain of the sampled-data system, respectively. The dynamic equations for the sampled-data model are:

$$\dot{\underline{x}}_s(t) = A\underline{x}_s(t) + B\underline{u}_s(kT), \quad \underline{x}_s(t_o) \text{ given} \tag{3-6}$$

$$\underline{u}_s(kT) = E(T)\underline{r}(kT) - G(T)\underline{x}_s(kT) \tag{3-7}$$

10

for $kT \le t \le (k+1)T$, $t_0 \le t$.

The A and B matrices in Eq. (3-6) are identical to those of Eq. (3-1). Substituting Eq. (3-7) into Eq. (3-6) yields

$$\underline{\dot{x}}_s(t) = A\underline{x}_s(t) + B[E(T)\underline{r}(kT) - G(T)\underline{x}_s(kT)] \tag{3-8}$$

for $kT \le t \le (k+1)T$.

The solution of Eq. (3-8) with $t = (k+1)T$ and $t_0 = kT$ is

$$\underline{x}_s[(k+1)T] = \left(e^{AT} - \int_{kT}^{(k+1)T} e^{A(kT+T-\tau)}d\tau \, BG(T)\right)\underline{x}_s(kT)$$

$$+ \int_{kT}^{(k+1)T} e^{A(kT+T-\tau)}d\tau \, BE(T)\underline{r}(kT) \tag{3-9}$$

The problem is to find $E(T)$ and $G(T)$ so that the states of the sampled-data model are as close as possible to that of the continuous-data system at the sampling instants, for a given input $r(t)$. Furthermore, in order that the solution for $E(T)$ is independent of $\underline{r}(t)$ it is necessary to assume that $\underline{r}(\tau) \cong \underline{r}(kT)$ for $kT \le t < (k+1)T$. Therefore, effectively, the input of the continuous-data system of Fig. 3-1 is assumed to pass through a sample-and-hold device. The above assumption would not affect the solution if $\underline{r}(\tau)$ has step functions as its elements. However, if the inputs are other than step functions, the approximation is a good one for small sampling periods.

Now letting $t_0 = kT$ and $t = (k+1)T$ in Eq. (3-4), and assuming $\underline{r}(\tau) \cong \underline{r}(kT)$ over one sampling period, we have

$$\underline{x}_c[(k+1)T] = e^{[A-BG(0)]T}\underline{x}_c(kT)$$

$$+ \int_{kT}^{(k+1)T} e^{[A-BG(0)](kT+T-\tau)}d\tau \, BE(0)\underline{r}(kT), \tag{3-10}$$

$kT \le t \le (k+1)T$.

11

The responses of Eq. (3-9) and Eq. (3-10) will match at $t = (k + 1)T$ for an arbitrary initial state $\underline{x}_c(kT)$ and an arbitrary input $\underline{r}(kT)$, if and only if the following two equations are satisfied:

$$e^{[A-BG(0)]T} = e^{AT} - \int_{kT}^{(k+1)T} e^{A[kT+T-\tau]} d\tau \, BG(T) \tag{3-11}$$

and

$$\int_{kT}^{(k+1)T} e^{A(kT+T-\tau)} d\tau \, BE(T)\underline{r}(kT) = \int_{kT}^{(k+1)T} e^{[A-BG(0)](kT+T-\tau)} d\tau \, BE(0)\underline{r}(kT) \tag{3-12}$$

Let $\lambda = (k + 1)T - \tau$. Then Eqs. (3-11) and (3-12) become

$$e^{[A-BG(0)]T} = e^{AT} - \int_{0}^{T} e^{A\lambda} d\lambda \, BG(T) \tag{3-13}$$

$$\int_{0}^{T} e^{A\lambda} d\lambda \, BE(T) = \int_{0}^{T} e^{[A-BG(0)]\lambda} d\lambda \, BE(0) \tag{3-14}$$

Eqs. (3-13) and (3-14) may be written in the simplified matrix form,

$$D(T) = - \theta(T)G(T) \tag{3-15}$$

and

$$\theta(T)E(T) = \theta_c(T)E(0) \tag{3-16}$$

where

$$D(T) = e^{[A - BG(0)]T} - e^{AT} \tag{3-17}$$

12

$$\theta(T) = \int_0^T e^{A\lambda} d\lambda B \tag{3-18}$$

$$\theta_c(T) = \int_0^T e^{[A-BG(0)]\lambda} d\lambda B \tag{3-19}$$

In Eqs. (3-15) and (3-16) if the number of unknowns equals the number of equations, $m = n$ and if $\theta(T)$ is nonsingular, then unique solutions of Eqs. (3-15) and (3-16) exist and are given by

$$G(T) = -\theta^{-1}(T)D(T) \tag{3-20}$$

and

$$E(T) = \theta^{-1}(T)\theta_c(T)E(0) \tag{3-21}$$

Generally speaking, the systems of equations of Eqs. (3-15) and (3-16) are not consistent for the case where $n > m$, and thus not all of the states of the continuous and sampled systems can be made to match at the end of each sampling period.

Although it is not possible to match all of the states it can be shown that it is possible to match some of the states or algebraic sums of the states at each sampling period. Multiplying both sides of Eq. (3-15) by a constant $m \times n$ matrix H gives,

$$HD(T) = -H\theta(T)G(T) \tag{3-22}$$

The above equation consists of mn scalar equations and mn unknowns. If H is chosen such that $H\theta(T)$ is nonsingular, Eq. (3-22) may be solved for a solution, $G_w(T)$,

$$G_w(T) = -[H\theta(T)]^{-1}HD(T) \tag{3-23}$$

Similarly, Eq. (3-16) may be solved for a solution $E_w(T)$,

$$E_w(T) = [H\theta(T)]^{-1}H\theta_c(T)E(0) \tag{3-24}$$

In general, the choice of the elements of H is governed by which combinations of the states are to be matched.

IV. Digital Redesign of the Wobble Dynamics

In this section the point-by-point method of digital redesign is applied to the

wobble dynamics of the spinning vehicle. If it is assumed that $\Gamma_3 = 0$, the state equations

for the wobble dynamics can be written as Eqs. (2-23)-(2-27).

The control vector for the continuous system is

$$\underline{u}_c = E(0)r - G(0)\underline{x}_c \tag{4-1}$$

where $E(0)$ and $G(0)$ represent the forward and feedback gains, respectively.

Two control postulates are investigated for this system. Using Control Law 1

and numerical values from Table 2-1, one obtains

$$G(0) = [0, -4.63, 0, -1.27, 0, 0], \quad E(0) = 1. \tag{4-2}$$

Control Law 2 requires feedback from each state and is written as

$$G(0) = [-1.263, 0.777, 0.172, -2.768, 1.792, 0.095], \quad E(0) = 1. \tag{4-3}$$

The control of the wobble dynamics is digitally redesigned with both control laws

and with $T = 0.2s$ and $H = [1, 1, 1, 1, 1, 1]$. The choice of H weighs all the states

equally and is natural for a single-input system. The gain matrices for the sampled-

data control system are obtained by using Eqs. (3-23) and (3-24), and are,

Control Law 1

$$G_w = [-0.0049, -3.95, 0.048, -1.08, -0.52, 0.0047], \quad E_w = 0.86. \tag{4-4}$$

Control Law 2

$$G_w = [-0.92, 0.456, 0.196, -2.14, 1.13, 0.09], \quad E_w = 0.728. \tag{4-5}$$

The continuous and sampled-data systems are simulated using both control laws.

It is found that in each case the states of the digital system closely match those of the

continuous system for this choice of sampling period. Figures 4-1 and 4-2 show the

state trajectories ϕ_1 and ϕ_2 for the continuous and sampled-data systems with Control Law 1.

14

V. Optimal Regulation and Digital Redesign of the Twelfth Order Model

In this section the twelfth-order model is optimally regulated and digitally redesigned by the point-by-point method of state comparison. The optimal regulation is achieved by calculating the optimal control law associated with the linear regulator design.

It has been determined that the overall system is uncontrollable with only one input to one of the wobble axes. When perturbed, the $\dot{\phi}_3$ state changes to a new value which means that the ϕ_3 state increases without bound as time increases. Since for spin about the 3-axis the ϕ_3 state is unimportant, only control of the $\dot{\phi}_3$ state is of importance. An additional input v_3 has consequently been provided to one of the spin axes to insure controllability. Since it is of interest to regulate only $\dot{\phi}_3$ and not ϕ_3 about their zero references, the state, ϕ_3, is deleted when calculating the optimal feedback gains.

The state equations for the twelfth-order model are given by Eqs. (2-19)-(2-22). These equations are reduced to an eleventh-order system by deleting the state ϕ_3. This system is optimized by the linear quadratic loss criterion for the following weighting matrices: $Q = I$, $R = I$. The 66th order algebraic Riccati equation associated with this problem is solved by the eigenvector method to yield the following feedback gains (10)

$$G(0) = \begin{pmatrix} -0.513 & 0.302 & -0.009 & -0.094 & -1.29 & -1.783 & .0820 & 0.0229 & 0.034 & 0.0021 & -0.457 \\ -0.043 & -0.053 & 0.93 & -1.82 & -0.0515 & -0.016 & -0.058 & -1.0 & 0.918 & 0.0043 & 0.0082 \end{pmatrix} \quad (5-1)$$

The digital redesign of this system is performed by use of the point-by-point method of partial matching. The weighting matrix H is chosen as

$$H = \begin{pmatrix} 1 & 1 & 0 & 0 & 1 & 1 & 1 & 0 & 0 & 0 & 1 \\ 0 & 0 & 1 & 1 & 0 & 0 & 0 & 1 & 1 & 1 & 0 \end{pmatrix} \quad (5-2)$$

and the feedback gains for the digital system are determined for two different sampling periods, $T = 0.2s$ and $T = 0.8s$. The choice of H is such that matching is obtained for the sum of the states of the wobble dynamics as well as the sum of the states of the spin

15

dynamics for each sampling instant. With $T = 0.2s$ the feedback gain matrix of the

sampled data system is

$$G_w = \begin{pmatrix} -0.442 & 0.183 & -0.011 & -0.0495 & -0.777 \\ -0.043 & -0.025 & 0.696 & -1.53 & -0.013 \end{pmatrix}$$

$$\begin{pmatrix} -1.41 & 0.450 & 0.0178 & 0.019 & 0.031 & -0.434 \\ -0.063 & -0.014 & -0.875 & 0.85 & 0.015 & 0.004 \end{pmatrix} \tag{5-3}$$

with $T = 0.8s$ the feedback matrix is

$$G_w = \begin{pmatrix} -0.332 & 0.095 & -0.0045 & 0.0055 & 0.128 & 0.775 \\ -0.032 & 0.026 & -0.0015 & -0.66 & -0.125 & -0.137 \end{pmatrix}$$

$$\begin{pmatrix} 0.21 & 0.006 & -0.0057 & 0.0017 & -0.22 \\ 0.066 & -0.51 & 0.548 & -0.009 & -0.025 \end{pmatrix} \tag{5-4}$$

The simulation of the 12th order model of the Spinning Skylab (Table 2-1) is performed with

each of the above gains. Figures 5-1 through 5-3 show the results with $T = 0.2s$. These

figures show the state trajectories for ϕ_1, ϕ_2, and ϕ_3. Figures 5-4 through 5-6 show the

state trajectories for ϕ_1, ϕ_2, ϕ_3 with $T = 0.8s$, and Figure 5-7 shows the control v_1 with

$T = 0.8s$. It is apparent that the point by point state comparison method of partial

matching yields acceptable redesign with $T = 0.2s$ as well as $T = 0.8s$.

IV. Conclusions

A practical onboard digital attitude control system for a class of spinning vehicles characterized by a rigid body and two connected flexible appendages has been designed and analyzed. A new approach to digital control system design, termed digital redesign, has been utilized. The simplicity of application of this approach is indicated by example. Whereas previously published reports have shown that the class of vehicles under consideration can be stabilized successfully with continuous-data control systems, this paper shows how that class of vehicles may in actual practice be stabilized and actively controlled with an onboard digital computer. A numerical example, using spinning Skylab parameters, has been utilized to substantiate the conclusions.

References

[1]Patel, J. S. and Seltzer., S. M., "Complex Eigenvalues Solution to a Spinning Skylab Program," NASA Tech. Memo. TM X-2378, Vol. II, "NASTRAN" Users' Experiences," Sept. 1971

[2]Patel, J. S. and Seltzer, S. M., "Complex Eigenvalue Analysis of Rotating Structures," NASA Tech. Memo. TM X-2637, "NASTRAN" Users' Experiences," Sept. 1972.

[3]Seltzer, S.M., Justice, D. W., Patel, J. S., and Schweitzer, G., "Stabilizing a Spinning Skylab," Proc. of the IFAC 5th World Congress, Paris, France, June 12, 1972.

[4]Seltzer, S. M., "Passive Stability of a Spinning Skylab," Journal of Spacecraft and Rockets, Vol. 9, No. 9, Sept. 1972, pp. 651-655.

[5]Seltzer, S. M., Schweitzer, G., and Asner, B., "Attitude Control of a Spinning Skylab," Journal of Spacecrafts and Rockets, Vol. 10, No. 3, March 1973, pp. 200-207.

[6]Chubb, W. B. and Seltzer, S. M., "Skylab Attitude and Pointing Control System," NASA TN D-6068, Feb. 1971.

[7]Seltzer, S. M., Patel, J. S., and Schweitzer, G., "Attitude Control of a Spinning Flexible Spacecraft," Computers & Electrical Engineering, Vol. 1, No. 3, Dec. 1973, pp. 323-340.

[8]Siljak, D. D., Nonlinear Systems, John Wiley & Sons, Inc., New York, 1969.

[9]Bullock, T. E. and Fosha, C. E., "A General Purpose FORTRAN Program for Estimation, Control, and Simulation, "Proceedings of the Eighth Annual IEEE Region III Convention, Huntsville, Alabama, Nov. 19-21, 1969.

[10]Potter, James, A., "Matrix Quadratic Solutions" J. Siam Appl. Math., Vol. 14, No. 3, May 1966, pp. 496-501.
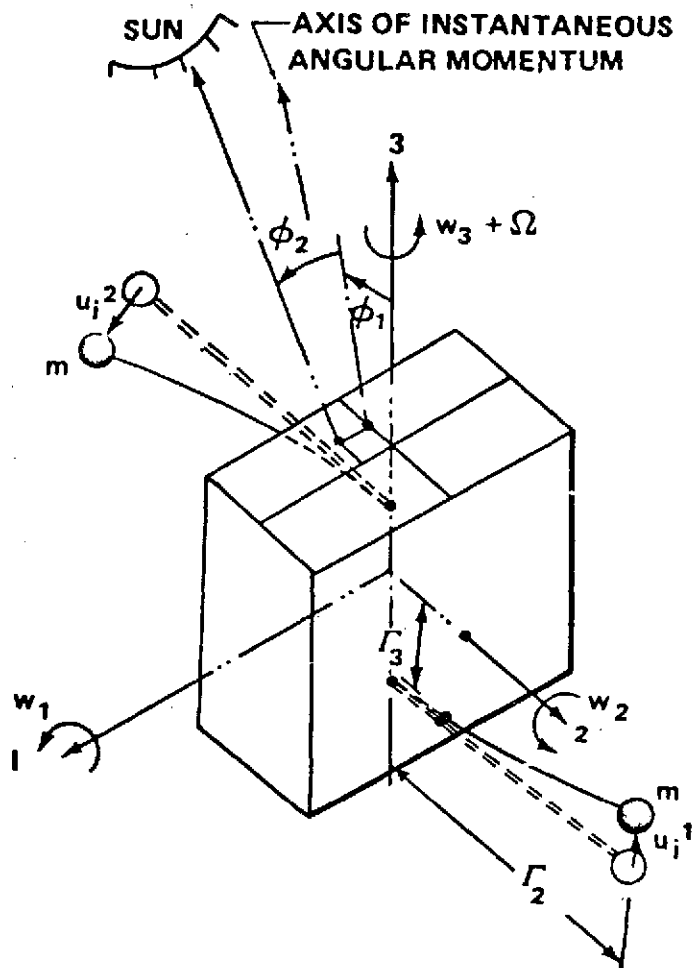
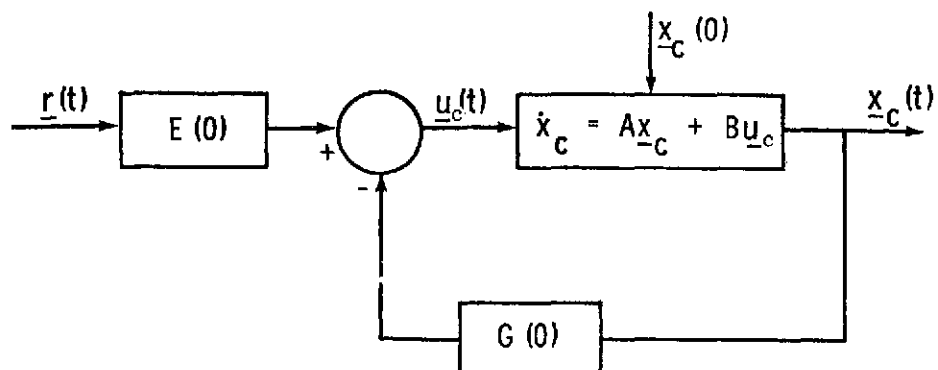Figure 1-1.   Model of Spinning Flexible Spacecraft.
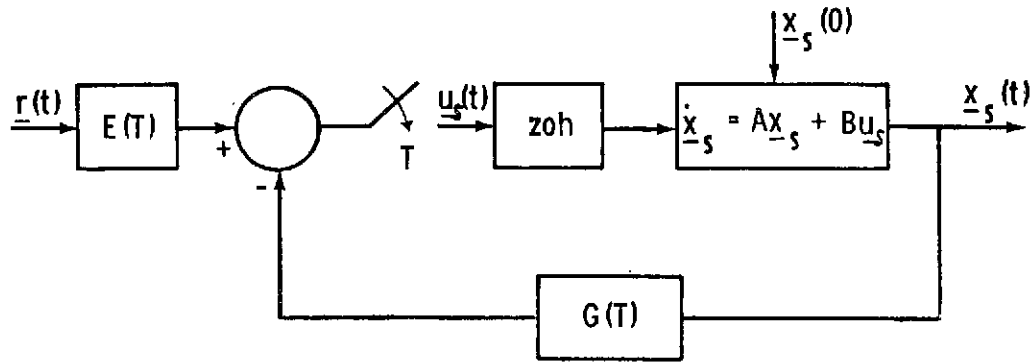

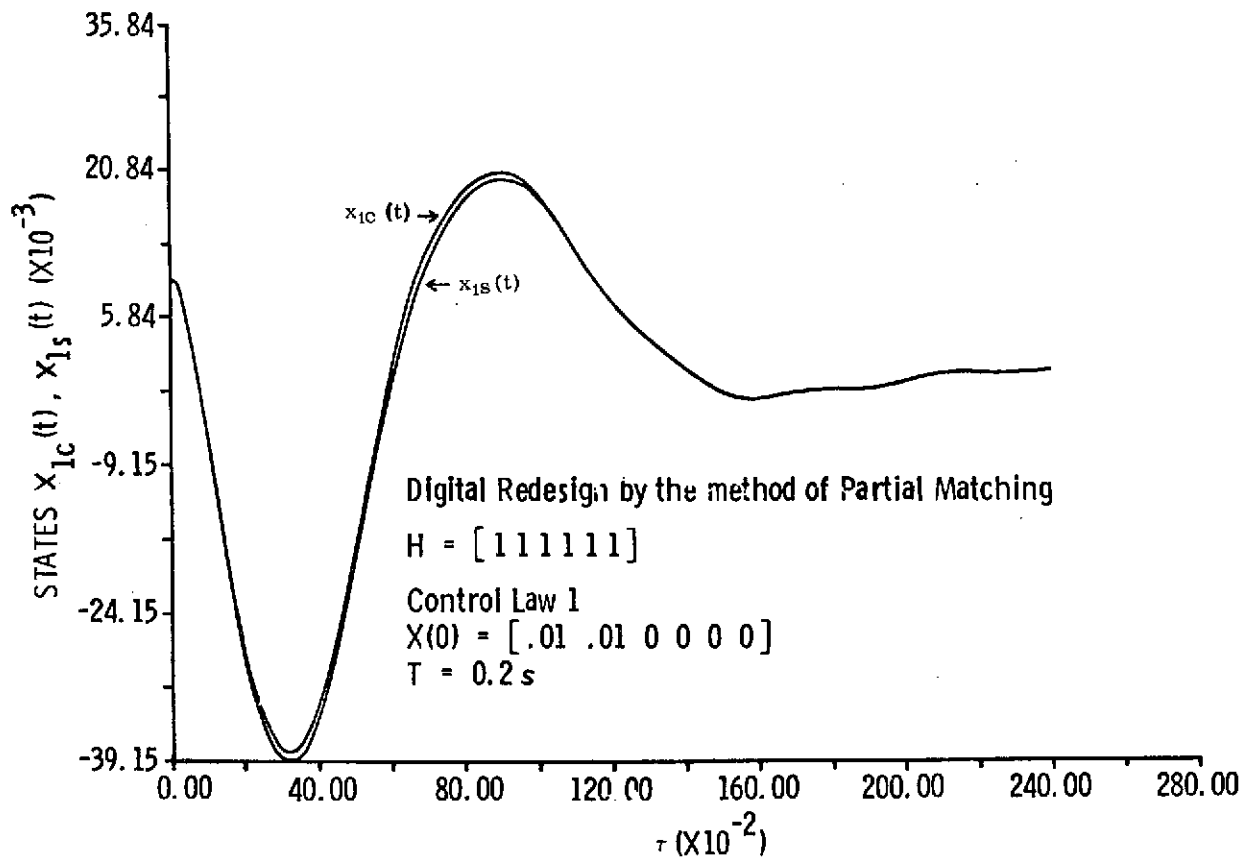Figure 3-1.   A Continuous-Data System.

Figure 3-2. A Sampled-Data System.

Digital Redesign by the method of Partial Matching

$H = \begin{bmatrix} 1 & 1 & 1 & 1 & 1 & 1 \end{bmatrix}$

Control Law 1
$X(0) = \begin{bmatrix} .01 & .01 & 0 & 0 & 0 & 0 \end{bmatrix}$
$T = 0.2 s$

Figure 4-1. State Trajectories $X_{1c}(t)$ and $X_{1s}(t)$ for the Wobble Dynamics of the Spinning Skylab.
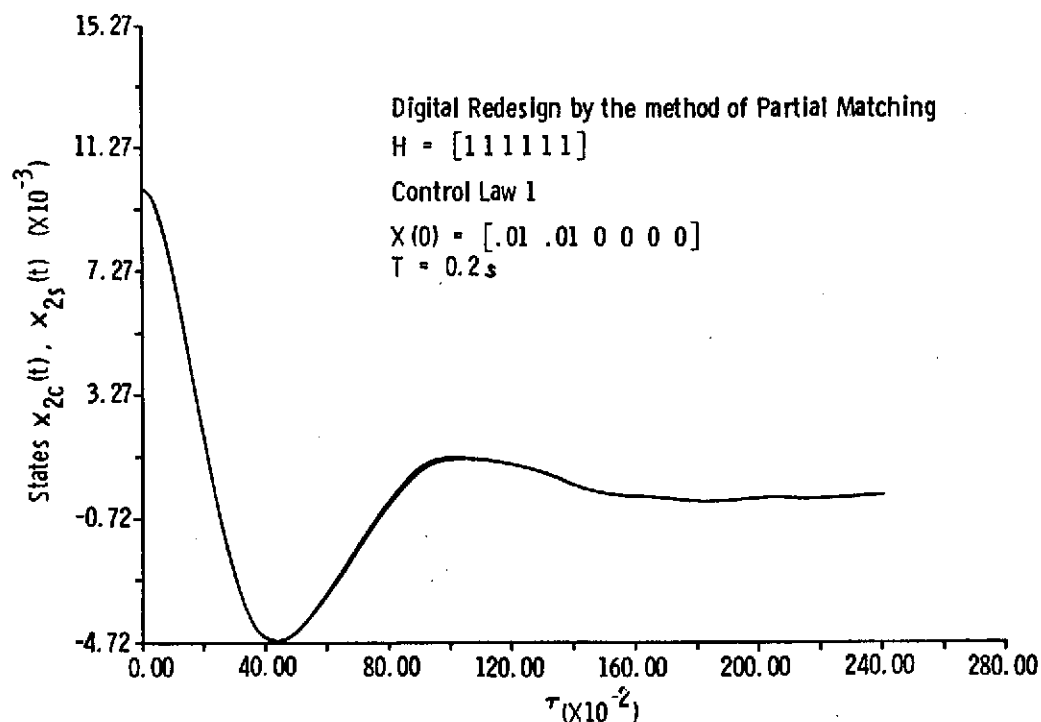
Figure 4-2. State Trajectories $X_{2c}(t)$ and $X_{2s}(t)$ for the Wobble Dynamics of the Spinning Skylab.
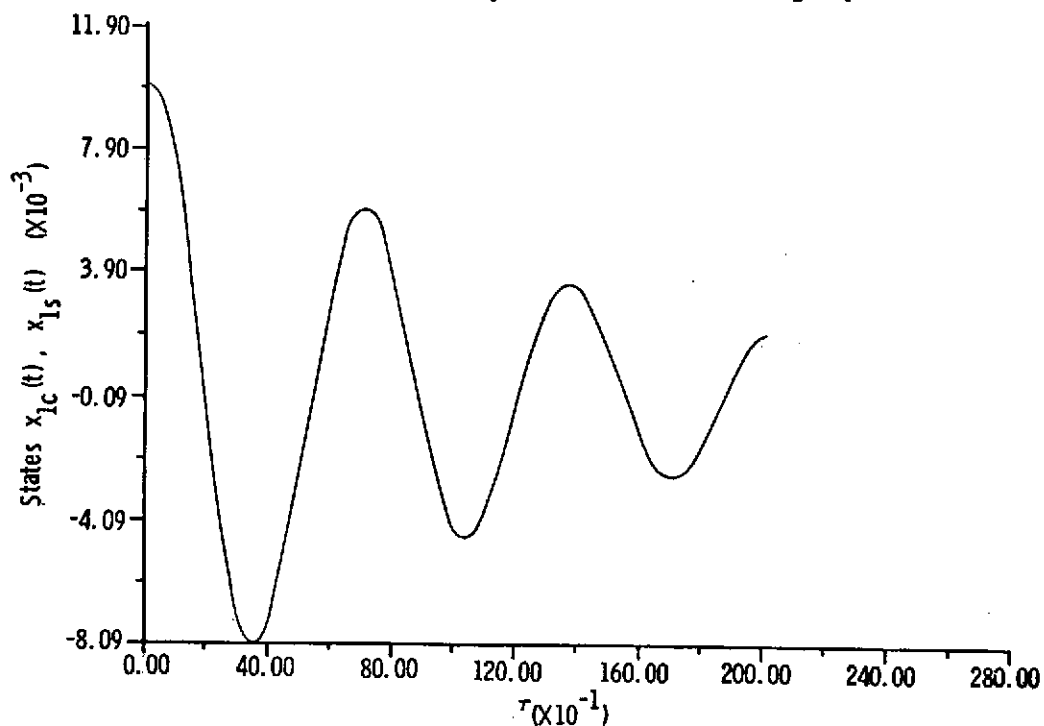
Figure 5-1. State Trajectories $X_{1c}(t)$ and $X_{1s}(t)$ for the 12th Order Model of the Spinning Skylab, Digital Redesign (T = 0.2s).
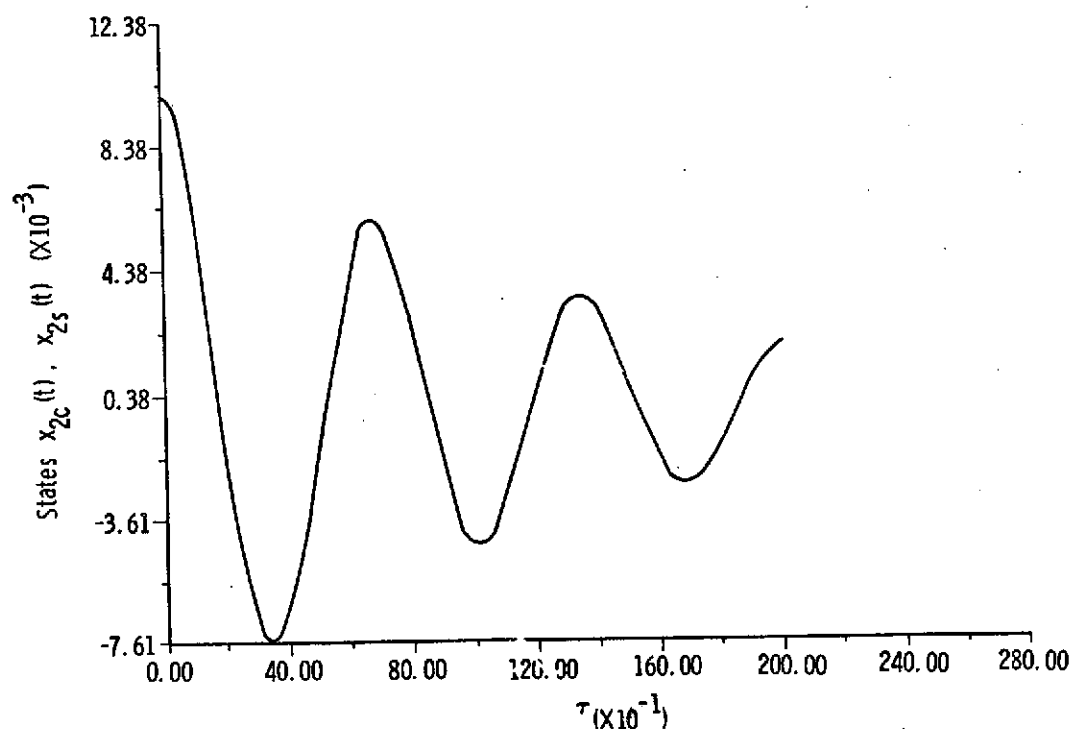
Figure 5-2. State Trajectories X_{2c}(t) and X_{2s}(t) for the 12th Order Model of the Spinning Skylab, Digital Redesign (T =0.2s)
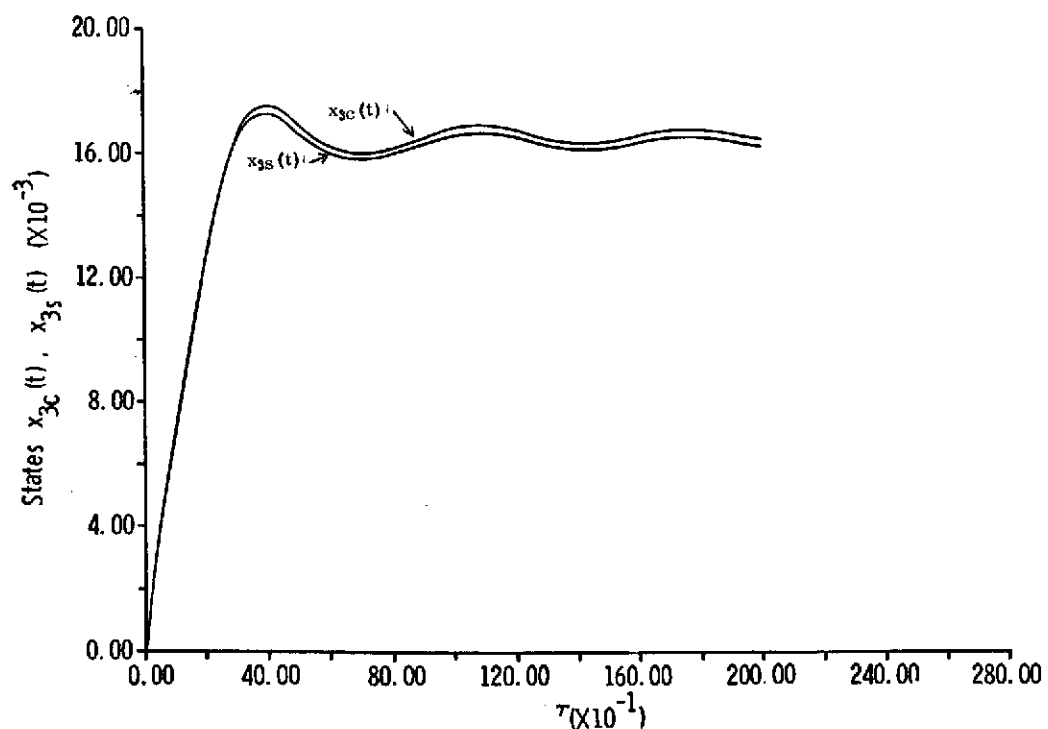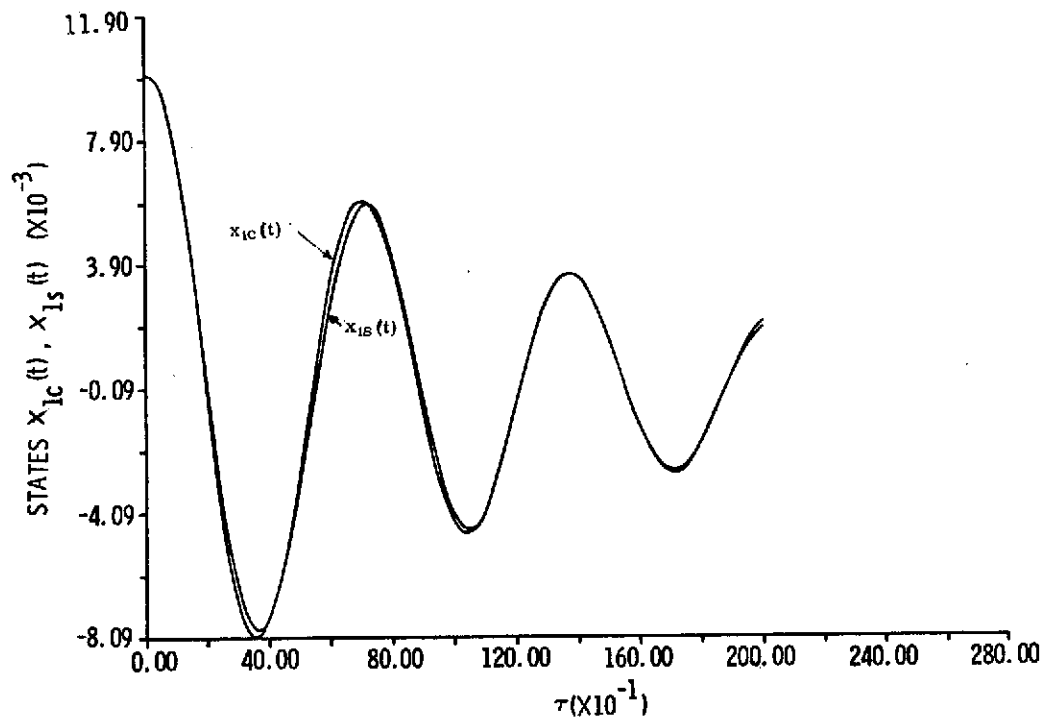

Figure 5-3. State Trajectories X_{3c}(t) and X_{3s}(t) for the 12th Order Model of the Spinning Skylab, Digital Redesign (T = 0.2s).

22

Figure 5-4. State Trajectories $X_{1c}(t)$ and $X_{1s}(t)$ for the 12th Order Model of the Spinning Skylab, Digital Redesign (T = 0.8s).
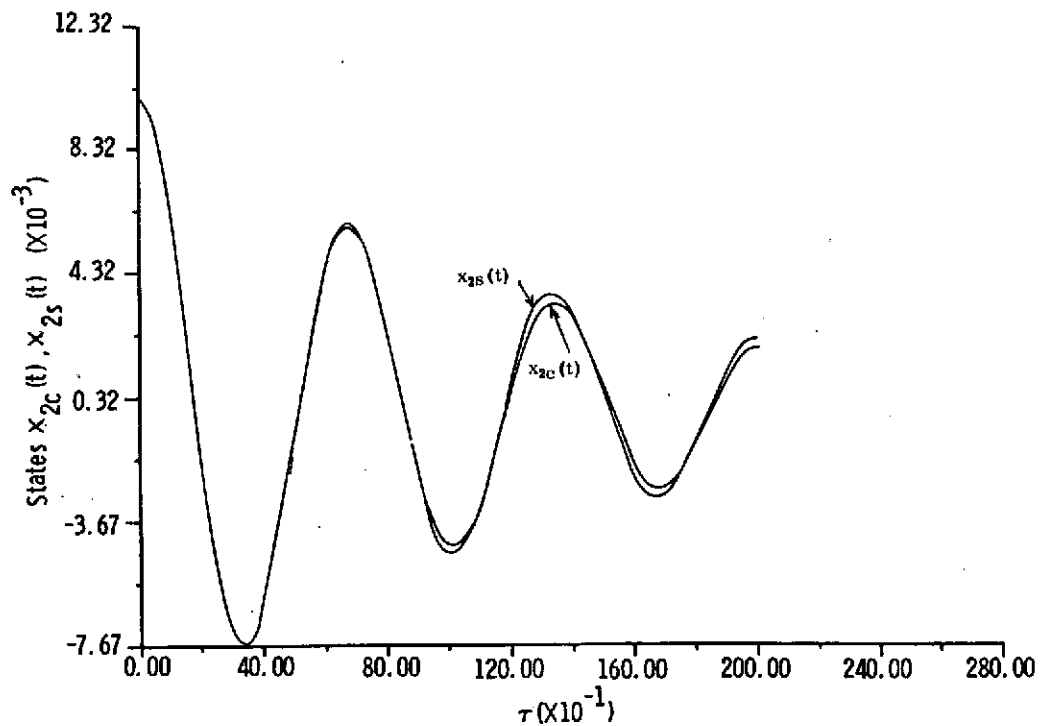

Figure 5-5. State Trajectories $X_{2c}(t)$ and $X_{2s}(t)$ for the 12th Order Model of the Spinning Skylab, Digital Redesign (T = 0.8s).
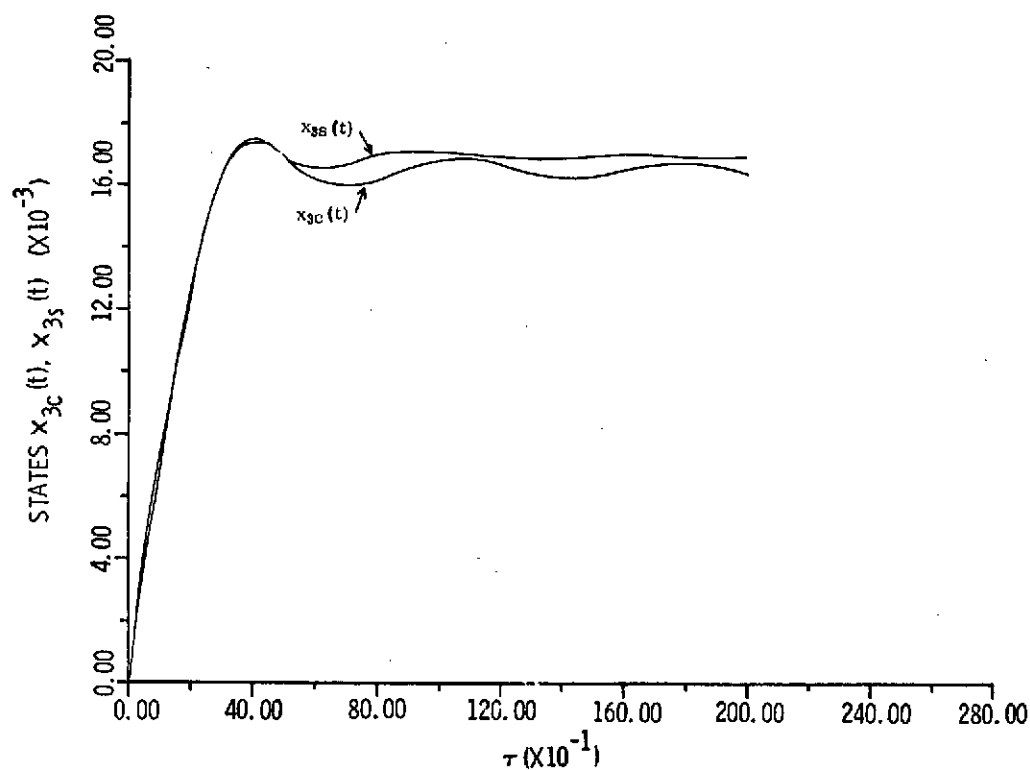
23

Figure 5-6. State Trajectories $X_{3c}(t)$ and $X_{3s}(t)$ for the 12th Order Mooef of the Spinning Skylab, Digital Redesign (T = 0.8s).
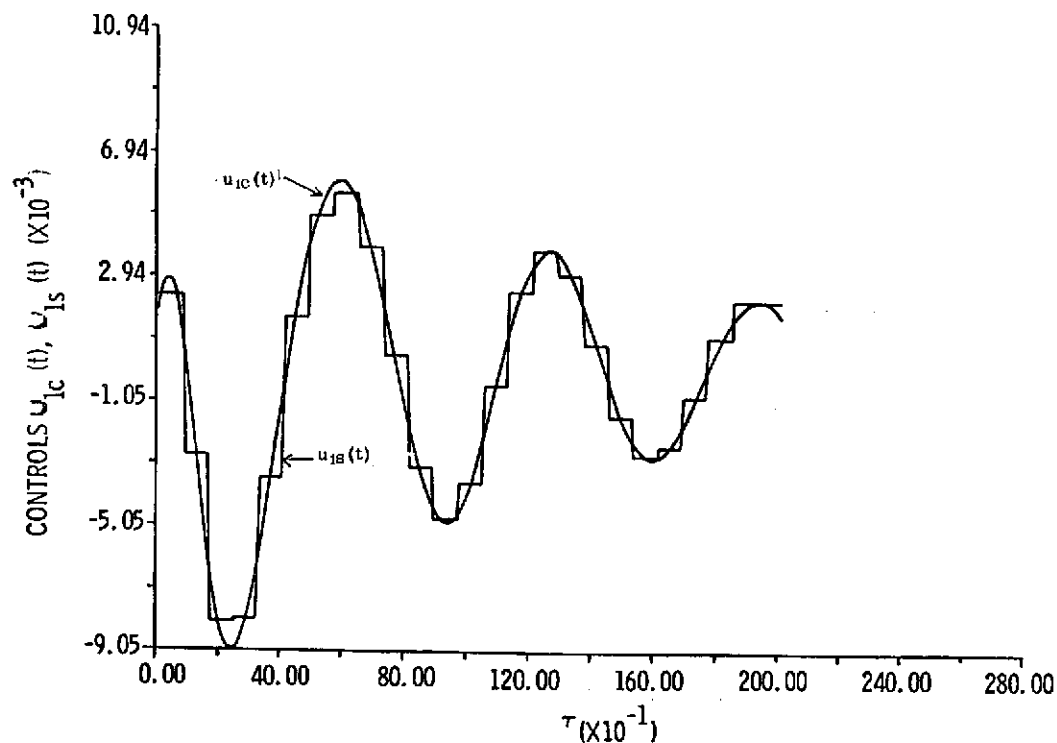

Figure 5-7. Control Trajectories $u_{1c}(t)$ and $u_{1s}(t)$ for the 12th Order Model of the Spinning Skylab, Digital Redesign (T = 0.8s).

APPROVAL

DESIGN OF A DIGITAL CONTROLLER FOR
SPINNING FLEXIBLE SPACECRAFT

By

B. C. Kuo, S. M. Seltzer, G. Singh, and
R. A. Yackel

The information in this report has been reviewed for security classification. Review of any information concerning Department of Defense or Atomic Energy Commission programs has been made by the MSFC Security Classification Officer. This report, in its entirety, has been determined to be unclassified.

This document has also been reviewed and approved for technical accuracy.

F. B. MOORE
Director, Astrionics Laboratory